

# Prediction and calculation of the shear creep behaviour of amorphous polymers under progressing physical ageing

Robert O. E. Greiner

*Siemens AG, Corporate Research and Technology, Base Technology Materials and Recycling, PO Box 3220, 91050 Erlangen, Germany*  
(Received 22 May 1992; revised 28 January 1993)

The shear creep behaviour of polystyrene PS N 7000 under the influence of physical ageing is thoroughly investigated. The theory of linear viscoelastic behaviour under the influence of ageing at constant temperature is briefly reviewed. Emphasis is given to the evaluation of the time-age shift function from creep experiments as well as to finding a suitable theoretical description of the time-age shift function and the creep behaviour. It has been shown that the multiparameter model based on free volume leads to an excellent description and prediction of the ageing behaviour in shear creep at constant temperature after various preconditioning times and at various ageing temperatures. Taking into account the history of the sample prior to the creep experiment, the creep behaviour under all given conditions is predicted from only one optional equilibrium creep curve.

(Keywords: physical ageing; shear creep; polystyrene volume recovery; free volume; multiparameter model)

## INTRODUCTION

In recent years great efforts have been made in investigating the ageing phenomenon of amorphous polymers. During ageing, many physical properties of a polymer change in the same manner as during cooling the material through its glass transition range. The polymer becomes stiffer and more brittle, its damping and creep rate decrease as do the specific volume and the free volume, dielectric constant, dielectric loss, etc.<sup>1-5</sup>. One of the first to describe these features in detail was Struik<sup>1</sup>. He called it physical ageing. He also elucidated the connection between physical ageing and volume recovery. Struik showed that many polymers age in the same way, and that the ageing behaviour in shear creep is influenced by temperature and loaded stress as well as by the ageing time. Based on the general viscoelastic theory for the non-isothermal case of Hopkins<sup>6</sup> and Haugh<sup>7</sup>, he proved that this theory and the mathematical formalism can be easily applied to the case of progressive ageing at constant temperature.

In some previous papers we have shown that the behaviour in volume of polymers can be well described under any thermal history using a multiparameter model<sup>4,8,9</sup> based on free volume<sup>10</sup>. It should be pointed out that the multiparameter model, developed by Hutchinson and Kovacs<sup>11</sup> was used here in its early version, where the partition parameter  $x$  equals zero, i.e. a full structural dependence of the retardation times was assumed. But the whole formalism is easily applied to values of  $x$  not equal to zero. Even in this simple version

the model will demonstrate its power in predicting viscoelastic deformation properties.

If the loss of free volume and mobility<sup>1</sup> is assumed to be the origin of the change in the creep properties during ageing, it seems worthwhile to follow this up. As a result of physical ageing, the viscoelastic deformation properties of polymers depend not only on loading history and temperature, but also on the progress of ageing prior to and during the loading period. Therefore the conventional technical mechanics of polymers, which is based on the concept of linear viscoelastic behaviour with a creep compliance depending on time and temperature only, must fail whenever ageing plays a significant role. Consequently the theory of viscoelastic behaviour of polymers should be generalized to include the influence of ageing.

Using the same multiparameter model as for the description of volume<sup>4,9,12</sup> we will examine and predict the creep behaviour of a commercial polystyrene (PS N 7000)<sup>10,12,13</sup> under various thermal histories, and the theoretical calculations will be compared with experimental data.

## THEORY OF VISCOELASTIC BEHAVIOUR UNDER THE INFLUENCE OF AGEING AT CONSTANT TEMPERATURE

In the following, consideration is restricted to the simple case of ageing at constant temperature. Although a detailed description of the theoretical fundamentals may

be found in the cited literature<sup>1,2,6,7,14</sup>, it is summarized briefly here since it provides several equations that are needed for understanding and discussion.

In the generalized non-isothermal theory of Hopkins<sup>6</sup> and Haugh<sup>7</sup> the linear viscoelastic behaviour of polymers in simple shear at constant temperature and prescribed stress history may be described by means of the deformation of a generalized Kelvin model. Now, in this model the elasticity of the springs and the viscosities of the dashpots are inserted as temperature-dependent functions.

A very simple result is obtained if thermorheologically simple behaviour is imposed on this mechanical model as an additional restriction. In this case, all spring constants of the model are temperature independent, whilst all viscosities have a similar temperature dependence. Assuming a temperature change from the reference temperature  $T_0$  to the temperature  $T$ , all viscosities are multiplied with the same factor  $a(T, T_0)$ , called the time-temperature shift factor<sup>15</sup>. For thermorheologically simple materials, the shear creep compliances  $J$  at the temperatures  $T$  and  $T_0$  have the same shape when plotted on a logarithmic time scale:

$$J(t, T) = J(t/a, T_0) \quad (1)$$

and may be brought into coincidence by a parallel shift along the logarithmic time scale. The amount of this shift is given by  $\log a(T, T_0)$ .

In the case of such a simple material behaviour, the non-isothermal strain response under a prescribed temperature history  $T(t)$  and under a prescribed stress history  $\sigma(t)$ , which does not start prior to  $t=0$ , is found as<sup>6,7</sup>:

$$\gamma(t) = J_0 \sigma(t) + \int_0^\lambda \dot{J}(\lambda - \xi) \sigma(\xi) d\xi \quad (2)$$

where  $\lambda$  is a function of time  $t$  and is called effective time. It may be calculated from the known time-temperature shift function,  $a$ , and the prescribed temperature history:

$$\lambda(t) = \int_0^t \frac{d\xi}{a(T(\xi), T_0)} \quad (3)$$

The effective time  $\xi$  is defined by the inverse function of equation (3).  $J_0$  and  $T_0$  are the values of the creep compliance and the prescribed temperature at  $t=0$ , respectively.

Equation (2) has the form of the ordinary superposition principle. However, the convolution integral is taken in the  $\lambda$ -time domain, whereas the stress history is inserted as a function of the effective time  $\xi$ . The creep rate at the temperature  $T_0$  is  $\dot{J}$ , which is taken as a function of the difference of the effective times  $\lambda$  and  $\xi$ . The case of non-isothermal creep of a thermorheological simple material is obtained if

$$\begin{aligned} \sigma[t(\lambda)] &= 0 & \text{for } \lambda < 0 \\ \sigma[t(\lambda)] &= \sigma_0 & \text{for } \lambda > 0 \end{aligned} \quad (4)$$

is inserted into equation (2) to give:

$$\gamma(t) = \sigma_0 J(\lambda, T_0) \quad (5)$$

where  $J(\lambda, T_0)$  has the meaning of creep function at constant temperature  $T_0$  as a function of the effective time  $\lambda$ . The relation between creep time,  $t$ , and effective time,  $\lambda$ , is given by equation (3).

All these considerations can be transferred immediately to the problem of viscoelastic behaviour under the

influence of ageing at constant temperature if the temperature is replaced by the degree of ageing,  $A$ , of the sample, which defines the time elapsed from the last quench from the equilibrium state down to the ageing temperature so far. The degree of ageing, also called the 'age' of the sample, has the dimension of a time. Furthermore, the time-temperature shift function  $a(T, T_0)$  is replaced by the time-age shift function  $b'(A, A_0)$ .

$J(t, A)$  is called the hypothetical course of the shear creep compliance as a function of the creep time,  $t$ , but at a fixed value for the degree of ageing,  $A$ . Generally this function will not be accessible experimentally since the degree of ageing cannot be kept constant during the measurement; however, referring to equation (1) we can write<sup>1</sup>:

$$J(t, A) = J(t/b', A_0) \quad (6)$$

Equation (6) relates the two creep functions at constant ages  $A$  and  $A_0$  to each other. Again, these two creep functions show the same shape on a logarithmic time scale, but are shifted over by the time-age shift function  $\log b'(A, A_0)$ . For the degree of ageing,  $A$ , at constant temperature we can write:

$$A(t) = t_e + t \quad (7)$$

where the preconditioning time,  $t_e$ , defines the time interval elapsed between the last quench from equilibrium to the ageing temperature and the beginning of the creep experiment;  $t$  is the instantaneous creep time. The effective time,  $\lambda$ , can then be expressed by:

$$\lambda(t) = \int_0^t \frac{d\xi}{b'(t_e + \xi, t_e)} \quad (8)$$

Equation (2) remains unchanged and  $\dot{J}$  now has the meaning of the creep rate of the hypothetical creep curve at the constant degree of ageing  $A = t_e$  (ref. 1).

The time dependence of temperature, shear stress and shear strain for a single quench is shown in Figure 1. The sample is quenched from a temperature above the glass transition temperature,  $T_g$ , down to the ageing temperature,  $T$ . After a preconditioning time  $t_e$  the sample is loaded with a constant stress,  $\sigma_0$ , and its strain,  $\gamma$ , is measured.  $\gamma$  will be proportional to  $\sigma_0$  and will depend on preconditioning time and creep time and we can write:

$$\gamma(\sigma_0, t, t_e) = \sigma_0 \tilde{J}(t, t_e) \quad (9)$$

where  $\tilde{J}$  now defines the creep compliance under the

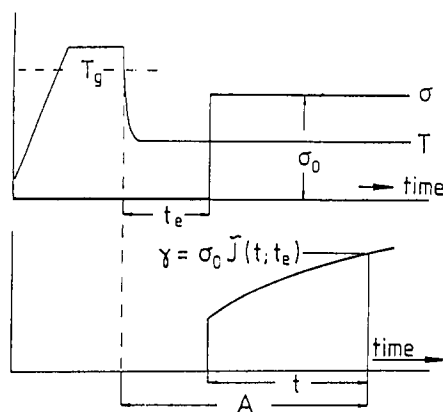
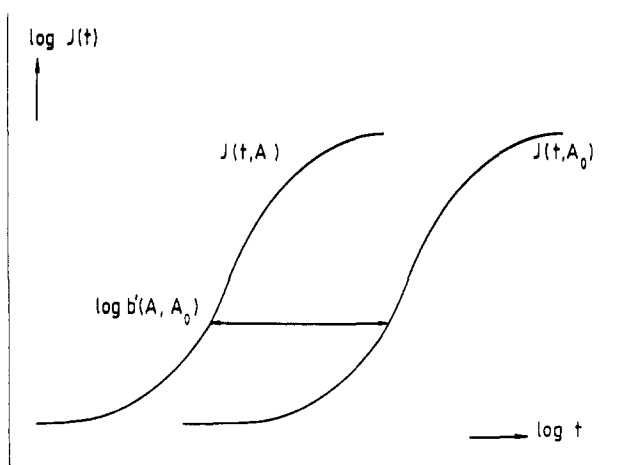


Figure 1 The course of temperature, stress and strain as functions of time



**Figure 2** Schematic presentation of two creep curves at constant but different ages  $A$  and  $A_0$

influence of progressive ageing, which is accessible by experiment. From equation (9) together with equation (5) we obtain:

$$\tilde{J}(t, t_e) = J(\lambda, t_e) \quad (10)$$

with  $\lambda$  as the effective time given by equation (8). Equation (10) means that the value of the measured creep compliance  $\tilde{J}(t, t_e)$  at the creep time  $t$  is the same as that of the hypothetical creep compliance  $J(\lambda, t_e)$  at the effective time  $\lambda$ , if the preconditioning time  $t_e$  is the same.

The meaning of the shift factor  $b'(A, A_0)$  at fixed degree of ageing  $A$  and  $A_0$  will become clear from *Figure 2* and the following consideration. If physical ageing is caused by volume recovery effects, the influence of ageing during long-time creep experiments at constant temperature cannot be ignored since, in contrast to temperature, the age of the sample cannot be kept constant during the measurements.

If it were possible to perform two creep measurements at different but fixed ages,  $A$  and  $A_0$ , the influence of these different amounts of ageing (equivalent to different preconditioning times  $t_e$ ) would only result in a parallel shift of the creep curves on the logarithmic time scale. The distance between the two curves is then  $b'(A, A_0)$ , as seen in *Figure 2*.

The construction of the creep compliance under progressive ageing,  $\tilde{J}(t, t_e)$ , from a creep compliance at constant age is discussed with reference to *Figure 3*. In this figure we have plotted schematically the measured creep compliance  $\tilde{J}(t, t_e)$  and two creep compliances at constant but different ages, namely  $A_0$  and  $A_\infty$ . The latter curves have the same shape and differ only in their position on the logarithmic time scale. The curve  $J(t, A_0)$  is the hypothetical creep curve that would be obtained, if the age of the sample could be fixed immediately after the beginning of the creep experiment, i.e.  $A_0$  is equal to the preconditioning time  $t_e$  and equation (7) can be written as:

$$A(t) = t_e + t = A_0 + t \quad (11)$$

In reality the shape of this creep curve is only measurable for creep times that are substantially smaller than the preconditioning time  $t_e$  (see equation (7)), according to Struik for  $t$  values smaller than  $0.1-0.3 t_e$ .

The curve  $J(t, A_\infty)$  represents the creep curve of a sample, for which the preconditioning time was chosen

to be long enough to reach the equilibrium state in volume before starting the creep experiment. Thus no further ageing could occur during the measurement. Finally  $\tilde{J}(t, t_e)$  is the shape of the creep curve starting after a preconditioning time  $t_e$  under progressive ageing. The experimental creep curve  $\tilde{J}(t, t_e)$  coincides with the hypothetical curve  $J(t, A_0)$  for short creep times ( $t \ll t_e$ ). When the creep time is of the order of  $t_e$ , a significant deviation from the shape of  $J(t, A_0)$  will arise. It will finally coincide again with the equilibrium creep curve  $J(t, A_\infty)$  after very long creep times ( $t \gg A_\infty$ ).

A straight line, drawn parallel to the logarithmic time axis, intersects the three curves at the times  $\lambda$ ,  $t$  and  $\mu$ . According to equation (10) we have by definition:

$$J(\lambda, A_0) = \tilde{J}(t, t_e) = J(\mu, A_\infty) \quad (12)$$

where  $\tilde{J}(t, t_e)$  is the measured creep compliance.

Replacing the preconditioning time  $t_e$  by  $A_0$  in equation (8) (cf. equation (11)) and after subsequent differentiation, we obtain:

$$\frac{d\lambda}{dt} = \frac{1}{b'(A_0 + t, A_0)} = \frac{1}{b'(A, A_0)} \quad (13)$$

or

$$\log b'(A, A_0) = -\log\left(\frac{\lambda}{t}\right) - \log\left(\frac{d \log \lambda}{d \log t}\right) \quad (14)$$

Let us assume that the shape of the equilibrium creep curve  $J(t, A_\infty)$  is known and the curve  $\tilde{J}(t, t_e)$  was measured. If  $J(t, A_\infty)$  is now shifted on the log-time axis until it coincides with the measured creep curve  $\tilde{J}(t, t_e)$  in the short-time region, then we have the hypothetical creep curve  $J(t, A_0)$  and  $\lambda$  may be determined as a function of  $t$  for all creep times investigated. Using equation (14), the time-age shift function  $b'(A, A_0)$  can be calculated. Otherwise we know from *Figure 3* and the preceding considerations that the following is valid:

$$\log b'(A_0, A_\infty) = \log \frac{\mu}{\lambda} = \log \frac{\mu}{t} + \log \frac{t}{\lambda} \quad (15)$$

and

$$\frac{d \log \lambda}{d \log t} = \frac{d \log \mu}{d \log t} \quad (16)$$

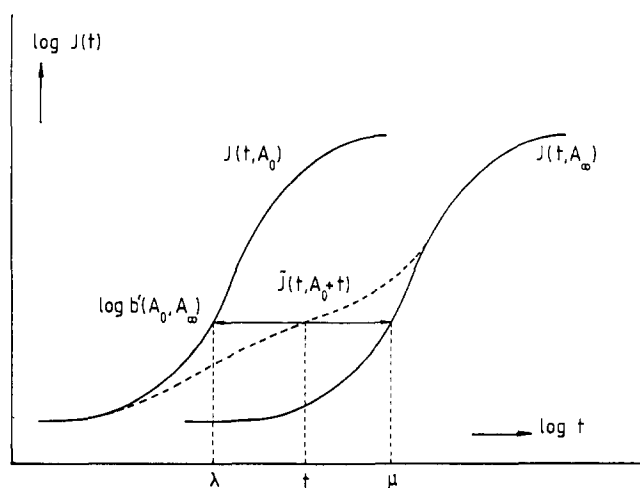


**Figure 3** Schematic course of creep curves at fixed age and during advancing ageing

Thus, assuming that the shape and the time position of the equilibrium creep curve  $J(t, A_\infty)$  are known as  $\tilde{J}(t, t_e)$  is measured, then we may determine  $\mu$  as a function of  $t$  for all creep times. For the time-age shift function we find:

$$\log b'(A, A_\infty) = \log \frac{\mu}{t} + \log \left( \frac{d \log \mu}{d \log t} \right) \quad (17)$$

This leads to the following important result. On the supposition that shape and time position of the equilibrium creep curve  $J(t, A_\infty)$  and the time-age shift function  $b'(A, A_\infty)$  are known at the ageing temperature, we can construct the shape of the creep curve  $\tilde{J}(t, t_e)$  at any preconditioning time  $t_e^{2,16-18}$ . But using this procedure we are always forced to determine the time-age shift function experimentally from very time-consuming ageing creep experiments.

Assuming now that these physical ageing effects that occur during creep measurements are due to the decrease of mobility of the polymer molecules and thus to the decrease in free volume, the time-age shift function must be directly related to the change in free volume.

In the multiparameter model<sup>4,8,9,11</sup>, the volume recovery behaviour can be expressed by the non-dimensional variable:

$$\delta = \frac{v - v_\infty}{v_\infty} \quad (18)$$

which measures the deviation of the fractional free volume,  $f$ , from its equilibrium value  $f_\infty$  according to:

$$f = \delta + f_\infty \quad (19)$$

In equation (18)  $v$  is the instantaneous and  $v_\infty$  the equilibrium value of the specific volume at a fixed temperature  $T$ .  $\delta$  may be divided into  $N$  different parts, related to  $N$  operating processes, to give:

$$\delta = \sum_{i=1}^N \delta_i \quad (20)$$

Each  $\delta_i$  is assumed to obey the basic Kovacs' equation<sup>3</sup>:

$$-\frac{d\delta_i}{dt} = \Delta\alpha_i \frac{dT}{dt} + \frac{\delta_i}{\tau_i} \quad (i=1, 2, \dots, N) \quad (21)$$

and the time dependence of the total deviation  $\delta$  is again obtained by summation over all  $i$  values:

$$\frac{d\delta}{dt} = \sum_{i=1}^N \frac{d\delta_i}{dt} \quad (i=1, 2, \dots, N) \quad (22)$$

In equation (21)  $\Delta\alpha_i$  represents the contribution of the  $i$ th process to the difference of the expansion coefficient in the rubbery,  $\alpha_r$ , and the glassy,  $\alpha_g$ , states:

$$\alpha_r - \alpha_g = \Delta\alpha = \sum_{i=1}^N \Delta\alpha_i \quad (i=1, 2, \dots, N) \quad (23)$$

and  $\tau_i$  is the  $i$ th retardation time, coupled with the  $i$ th process and is given by:

$$\tau_i = \tau_{i,r} \exp \left( \frac{b}{f} - \frac{b}{f_r} \right) \quad (i=1, 2, \dots, N) \quad (24)$$

where  $\tau_{i,r}$  and  $f_r$  are the retardation time and the free volume at a reference temperature  $T_r$ . The retardation times  $\tau_i$  in equation (24) are allowed to depend both on temperature  $T$  as well as on the instantaneous state of the sample, defined by  $\delta$ . This is obvious if equation (24)

**Table 1** Material parameters for PS N 7000 o.W. used for the calculations

$c_1 = 10$	$\tau_1 = 5 \times 10^{-6} \text{ s}$	$g_1 = 0.100$
$c_2 = 39.5 \text{ K}$	$\tau_2 = 2 \times 10^{-4} \text{ s}$	$g_2 = 0.070$
$T_r = 105^\circ \text{C}$	$\tau_3 = 1.75 \times 10^{-2} \text{ s}$	$g_3 = 0.110$
$\alpha_1 = 5.66 \times 10^{-4} \text{ K}^{-1}$	$\tau_4 = 3 \times 10^{-1} \text{ s}$	$g_4 = 0.170$
$\alpha_2 = 1.76 \times 10^{-4} \text{ K}^{-1}$	$\tau_5 = 6 \times 10^{-1} \text{ s}$	$g_5 = 0.165$
$\alpha = 3.90 \times 10^{-4} \text{ K}^{-1}$	$\tau_6 = 8 \text{ s}$	$g_6 = 0.385$

The  $g_i$ s are the normalized intensities of the retardation spectrum<sup>4</sup>

is transformed as follows:

$$\tau_i(T, \delta) = \tau_{i,r} \exp \left( \frac{b}{f_\infty} - \frac{b}{f_r} \right) \exp \left[ -\frac{b\delta}{f_\infty(f_\infty + \delta)} \right] \\ = \tau_{i,r} a_T a_\delta \quad (i=1, 2, \dots, N) \quad (25)$$

In equation (25)  $f_r$  and  $\tau_{i,r}$  denote the value of the free volume and the value of the  $i$ th retardation time at the reference temperature  $T_r$ , respectively, whilst  $f_\infty$  denotes the equilibrium value of the free volume at the ageing temperature  $T_a$ .  $b$  is a constant of the order of one and is not to be confused with the time-age shift function  $b'$  (see equations (14) and (17)).  $b$  can be calculated if the Williams-Landel-Ferry constants  $c_1$ ,  $c_2$  and  $\Delta\alpha$  are known (see Table 1)<sup>4,9,10,15</sup>. The shift factor  $a_T$  characterizes the temperature dependence of the retardation times and the second exponential term in equation (25),  $a_\delta$ , reveals the influence of the instantaneous state of the system and is dependent on the prior history and the degree of ageing of the sample.

Regarding now a volume recovery experiment and a creep experiment under progressive ageing at the same temperature, the shift functions  $a_\delta$  and  $b'(A_\infty, A)$  should be comparable if the prehistories are approximately the same and the change in free volume is the origin of ageing effects.

## EXPERIMENTAL AND RESULTS

All creep measurements were performed with a commercial polystyrene PS N 7000 o.W. The abbreviation o.W. refers to the sample preparation and stands for softening under vacuum, therefore the sample no longer contains any lubricant. All creep measurements were performed in torsion and the creep compliance,  $\tilde{J}(t)$ , was measured at small stresses ( $< 20 \text{ kPa}$ ) and strains ( $< 1\%$ ); i.e. only the range of linear creep behaviour is considered here<sup>2,13</sup>. A detailed description of the material used and the experimental techniques are given elsewhere<sup>2,9,13,18-22</sup>. This paper is restricted to the presentation of some experimental results and important comments necessary for their understanding and interpretation.

Prior to the creep experiment, the sample was always cooled from the equilibrium state at  $115^\circ \text{C}$  to the ageing temperature  $T_a$  by natural cooling. At a temperature of  $T_a + 6 \text{ K}$ , counter-heating is started to reach a smooth approach to the ageing temperature. Thus for cooling the last 6 K, about 6 min is necessary whatever the value of  $T_a$ . This is an important fact since, depending on the ageing temperature, the sample is cooled through the glass transition range at different rates. The higher the value of  $T_a$ , the lower the cooling rate and the lower the value of the free volume which is frozen in at the glass transition temperature  $T_g$ . These different prehistories

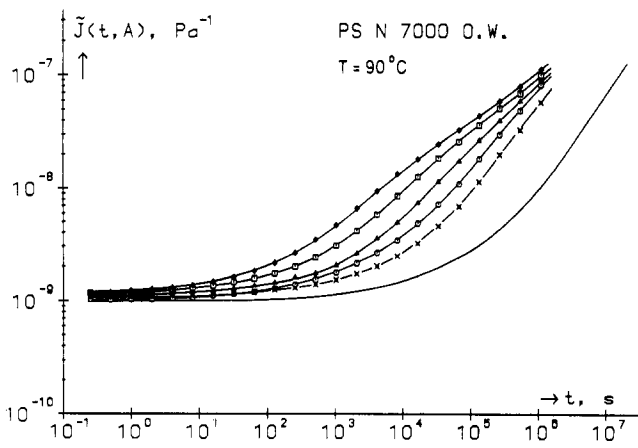


**Figure 4** Creep curves of PS N 7000 under the influence of progressive ageing at  $T_a = 90^\circ\text{C}$  after various preconditioning times:  $t_e = 2^{11}$  s ( $\diamond$ );  $2^{13}$  s ( $\square$ );  $2^{15}$  s ( $\triangle$ );  $2^{17}$  s ( $\circ$ );  $2^{19}$  s ( $\times$ ). The full line represents the equilibrium creep curve at  $90^\circ\text{C}$

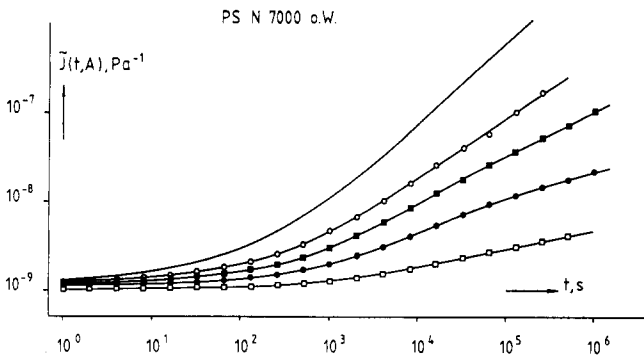


**Figure 5** Creep curves of PS N 7000 under the influence of progressive ageing after a preconditioning time  $t_e = 2^{13}$  s at various ageing temperatures:  $T_a = 92.5^\circ\text{C}$  ( $\circ$ );  $90^\circ\text{C}$  ( $\blacksquare$ );  $85^\circ\text{C}$  ( $\bullet$ );  $70^\circ\text{C}$  ( $\square$ ). The full line represents the equilibrium creep curve at  $95^\circ\text{C}$

have to be considered in the theoretical calculations and we will come back to this fact in detail.

Figure 4 shows creep measurements on PS N 7000 at the ageing temperature of  $T_a = 90^\circ\text{C}$ <sup>20</sup>. Upon completion of the different preconditioning times indicated, the creep experiments were started. The full curve represents the measured equilibrium creep curve, where the preconditioning time chosen was long enough (about 4 months) to reach equilibrium in volume.

All the ageing creep curves have a similar form, as shown schematically in Figure 3. At short creep times they have the form of the equilibrium creep curve with positive curvature. When the creep time reaches values between 0.1 and 0.3  $t_e$ , as ageing proceeds the creep curves deviate from the equilibrium creep curve in the direction of smaller deformations. They show a continuously decreasing slope,  $d \log \bar{J}(t)/d \log t$ , until the creep time reaches the preconditioning time necessary for obtaining equilibrium in volume. Then the creep curves show a positive curvature again and finally all curves converge to the equilibrium creep curve.

A remarkable feature of these creep curves is the different initial plateaux at short creep times. With increasing preconditioning time,  $t_e$ , the creep compliance is shifted to lower values in the short-time region. It was exactly this behaviour that was pointed out in detail by

Struik<sup>1</sup>. As a first consequence it means that the creep curves in the short-time region, although still having the shape of the equilibrium creep curve, cannot be brought to coincidence merely by a horizontal shift parallel to the logarithmic time axis; an additional vertical shift is necessary.

A second set of creep measurements is shown in Figure 5<sup>20</sup>. Again, prior to the creep experiment the sample was cooled down from the equilibrium state at  $115^\circ\text{C}$  by natural cooling but to various ageing temperatures  $T_a$ . Then the creep measurements were started after identical elapsed preconditioning times  $t_e = 2^{13}$  s. We observe a similar creep behaviour as in Figure 4, but now in the short-time region the  $\bar{J}(t)$  curves show a temperature-dependent initial plateau, i.e. with decreasing ageing temperature the creep compliance is shifted to lower values and the whole curve is shifted to longer times on the creep time axis. Here, too, the curves cannot be brought to coincidence by only horizontal shifting, an additional vertical shift is necessary.

## DISCUSSION

From Figures 4 and 5 we get some indications that for a theoretical description it is necessary to find an expression regarding the time-age and the time-temperature dependence of the creep compliance.

We start analysing the creep behaviour at constant temperature and various preconditioning times  $t_e$  as shown in Figure 4. Disregarding provisionally the short-time region and determining the time-age shift function  $b'(A_\infty, A)$  according to equation (17) for creep times longer than 0.1  $t_e$ , we get the shape shown in Figure 6 (full points) if  $b'(A_\infty, A)$  is plotted versus the degree of ageing,  $A$ , (cf. equation (7)) of the sample<sup>2</sup>. The equilibrium creep curve<sup>18</sup> in Figure 4 was chosen as reference creep curve. Also shown in Figure 6 is the shift function  $a_\delta$ , calculated theoretically from equation (25) according to:

$$a_\delta = \exp \left[ - \frac{b\delta}{f_\infty(f_\infty + \delta)} \right] \quad (26)$$

and using the parameters of the multiparameter model from Table 1. In the calculation of  $a_\delta$  it was considered that, prior to the creep experiment, the sample was cooled down through the glass transition range at a rate of

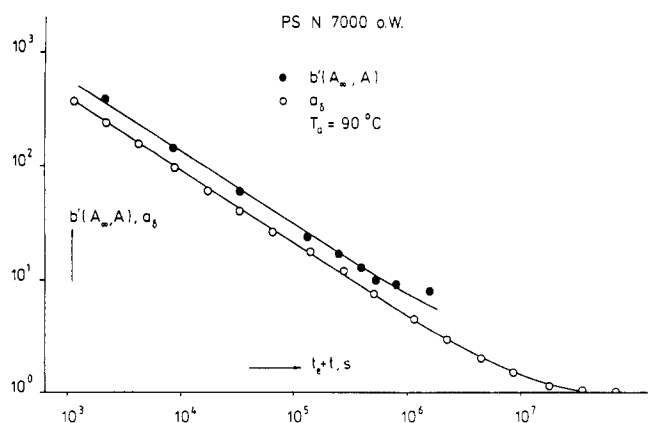


**Figure 6** Presentation of the shift functions  $b'(A_\infty, A)$  and  $a_\delta$  determined from creep measurements and calculated by means of the multiparameter model, respectively

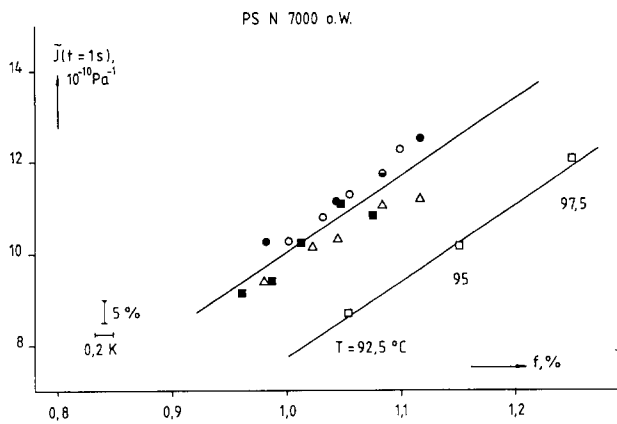


Figure 7 Measured  $\tilde{J}(t=1\text{ s})$  values plotted against calculated free volume values for various prehistories:  $\circ$ ,  $T_a=90^\circ\text{C}$  and  $t_c=2^{11}, 2^{13}, 2^{15}, 2^{17}, 2^{19}\text{ s}$ ;  $\blacksquare$ ,  $T_a=85^\circ\text{C}$  and  $t_c=2^{11}, 2^{13}, 2^{15}, 2^{17}, 2^{19}\text{ s}$ ;  $\triangle$ ,  $\bullet$ ,  $t_c=2^{13}\text{ s}$  and  $T_a=92.5, 90, 85, 80, 70, 60^\circ\text{C}$ ;  $\square$ , equilibrium values at  $T_a=97.5, 95, 92.5$

approximately  $1.5^\circ\text{C min}^{-1}$  (refs 9, 20). The changes in  $\delta$ , and thus in free volume, during the cooling period were calculated by using equations (18) to (25), assuming a linear cooling rate:

$$-q = \frac{dT}{dt} \quad (27)$$

Consequently the actual state of the sample immediately before starting the creep experiment is known, and the changes in free volume during the creep measurement at constant temperature are characterized by the changes of  $a_\delta$ . A detailed description of the method of calculation is given in refs 4 and 9.

Apart from some difference in the time position, both functions show the same linear dependence on the age of the sample in the overlapping time interval. In contrast to  $b'(A_\infty, A)$ , the shape of  $a_\delta$  can easily be calculated up to the equilibrium state in volume, which is reached when  $a_\delta$  is unity. The slight time difference between the two shift functions is due to the time position of the reference equilibrium creep curve chosen for the determination of  $b'(A_\infty, A)$ . In Figure 4 this position is about  $1.5 \times 10^7\text{ s}$  for the creep compliance value of  $\tilde{J}(t) = 10^7\text{ Pa}^{-1}$ . Due to the long preconditioning and the long creep time, the exact position of this curve on the time scale may be somewhat uncertain. If the time of  $1.5 \times 10^7\text{ s}$  is reduced to  $1 \times 10^7\text{ s}$ , the two curves in Figure 6 coincide.

The necessity of finding an adequate reduction method for bringing to coincidence the different initial plateaux of the creep compliance for creep times smaller than  $0.1 t_c$  is obvious if we try to construct the function  $b'(A_\infty, A)$  from Figure 5. Due to the extremely flat shape of the creep curves at low temperatures, the time-age function without vertical shift is only accessible at long creep times, for example at  $70^\circ\text{C}$  for creep times longer than  $10^4\text{ s}$ .

A further problem arises in measuring the equilibrium creep curves at low ageing temperatures, which has to be done if  $b'(A_\infty, A)$  is to be determined according to equation (17). In ref. 4 it is shown that the equilibrium state in volume can be reached within a reasonable experimental time scale only for temperatures near  $T_g$ . Thus the preconditioning time for the equilibrium creep curve at  $T_a=90^\circ\text{C}$  is about 4 months, at  $85^\circ\text{C}$  about 30 years (calculated<sup>4,9</sup>) and at  $70^\circ\text{C}$  it would be thousands of years.

The latter problem is solved since it has been shown in ref. 2 that for the evaluation of the time-age shift function it is not absolutely necessary to know the exact time position of the equilibrium creep curve, but it is sufficient to know the shape of the equilibrium creep curve.

The problem of the reduction of the  $\tilde{J}(t)$  curves in the short-time region still remains. In Figures 4 and 5 the variation of the  $\tilde{J}(t)$  values at short creep times with  $t_c$  and  $T_a$ , respectively, is about 15–20% in the interval of interest. The only quantity that can be used to explain this strong time and temperature dependence of the creep compliance is the free volume. Other reduction methods<sup>14,23</sup>, as for example  $Q/T/Q_0 T_0$ , lead only to a variation of about 1%.

In Figure 7 the  $\tilde{J}(t)$  values from Figures 4 and 5 after creep times of 1 s are plotted against the corresponding free volume values calculated by means of the multiparameter model, with respect to the various temperature prehistories (see equations (18)–(25)).  $\tilde{J}(t=1\text{ s})$  values are also shown in this figure, but are not discussed here<sup>18,20,21</sup>. Apart from the absolute values characterizing the equilibrium creep compliance (open squares) at the ageing temperatures  $T_a=92.5, 95$  and  $97.5^\circ\text{C}$ , we find for all  $\tilde{J}(t=1\text{ s})$  values approximately the same dependence on the free volume. All the ageing creep values can be described by the same straight line if tolerances of 5% in  $\tilde{J}(t)$  and  $\pm 0.2^\circ\text{C}$  in the temperature are assumed.

Taking as a base a known reference value  $\tilde{J}_r(1\text{ s})$  and the corresponding value of the free volume  $f_r$  we can calculate any  $\tilde{J}(1\text{ s})$  value from the equation:

$$\tilde{J}(1\text{ s}) = \tilde{J}_r(1\text{ s}) + m(f - f_r) \quad (28)$$

where the slope  $m$  is  $1.5 \times 10^{-7}\text{ Pa}^{-1}$ .

The ageing creep curves from Figure 4 ( $T_a=90^\circ\text{C}$ ) reduced according to equation (28) are shown in Figure 8. As reference value  $\tilde{J}_r(1\text{ s})$  the 1 s value of the creep curve with a preconditioning time  $t_c=2^{13}\text{ s}$  was chosen. We observe that all creep curves coincide in the short-time region. For creep times greater than  $0.3 t_c$  the influence of the reduction vanishes and the  $\tilde{J}(t)$  values are almost the same as shown in Figure 4. These creep curves can now be evaluated by traditional methods<sup>2,16,17</sup> and the shift function  $b'(A_\infty, A)$  can be determined even in the short-time region.

The same procedure is now applied to the creep curves at different ageing temperatures shown in Figure 5. First,

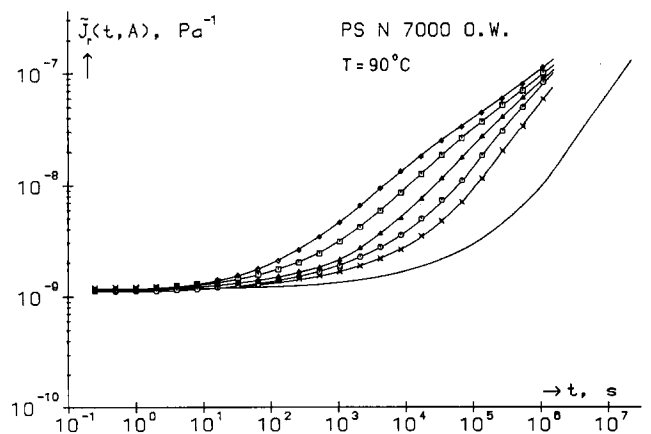


Figure 8 Creep curves from Figure 4, reduced according to equation (28)

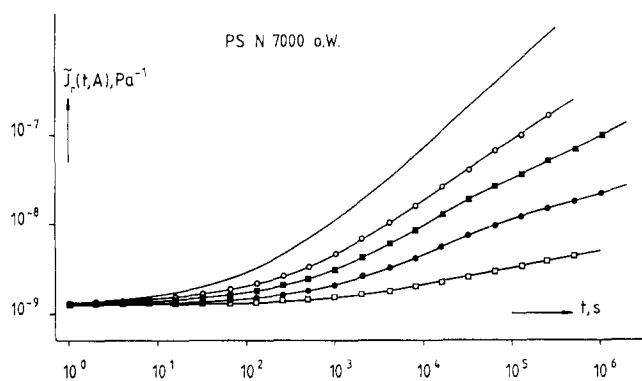


Figure 9 Creep curves from Figure 5, reduced according to equation (28)

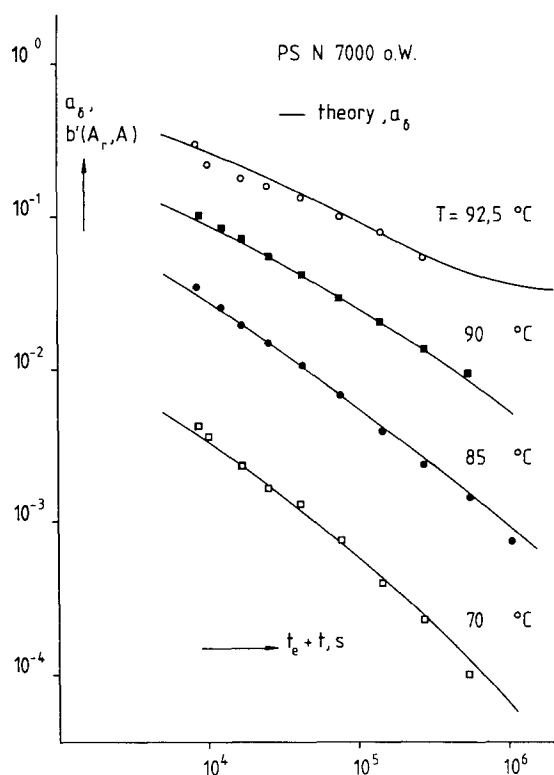


Figure 10 Presentation of the shift functions  $b'(A_r, A)$  and  $a_\delta$  determined from creep measurements and calculated by means of the multiparameter model, respectively

reduction by means of equation (28) was performed, whereby the  $\bar{J}(1\text{ s})$  value of the creep curve at 90°C was chosen as the reference value, and then the construction of the shift function from these reduced curves is carried out. The reduced creep curves of Figure 5 are shown in Figure 9. Again, we note that really good coincidence of the curves is obtained in the short-time region by applying equation (28).

The resulting time-age shift functions  $b'(A_r, A)$  constructed from Figure 9, are shown in Figure 10. The index  $r$  at  $A_r$  indicates that the real equilibrium creep curve at each ageing temperature was not used; instead for all creep curves the equilibrium creep curve of 95°C was selected as the reference curve. In contrast to Figure 6 where the time-age shift function takes positive values, the shift functions in Figure 10 have negative values. This effect is due to the different time position of

the reference equilibrium creep curve with respect to the ageing creep curves. Apart from this fact, the shape of the time-age functions is similar. Depending on the ageing temperature, the time-age function is shifted to more and more negative values and the slope of the curves increases slightly with decreasing temperature. For comparison, the calculated  $a_\delta$  functions are shown in the same figure as solid lines. Both shift functions show excellent agreement over the whole time interval considered. As mentioned, for the theoretical calculations it is important to take into account the different temperature histories prior to the creep measurements. In Table 2 the estimated cooling rates used for the calculation are given for each ageing temperature. In the present case the temperature history is approximated by linear cooling through the glass transition range, but further improvement may be achieved by simulating the true natural cooling, which is easily done by assuming an exponential decay for the cooling rate in equations (27) and (21).

Summarizing the results so far, the multiparameter model based on free volume leads to a good description of the time-age shift function as well as to a good reduction of the creep curves in the short-time region under various thermal prehistories. It should now be possible to predict ageing creep curves at various preconditioning times and ageing temperatures from only one known, optional equilibrium creep curve by using the multiparameter model together with the parameters of Tables 1 and 2. The results are presented in Figures 11 and 12. The calculations were performed applying the following scheme:

1. choice of any known equilibrium reference creep curve;
2. calculation of the vertical shift by means of equation (28);

Table 2 Estimated cooling rates

$T_a$ (°C)	$-q$ (°C s <sup>-1</sup> )
92.5	0.005
90.0	0.025
85.0	0.080
70.0	0.25

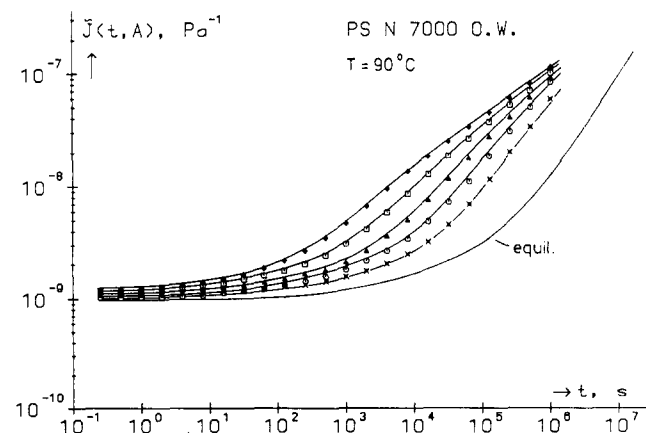


Figure 11 Comparison between experiment (symbols) and theory (drawn lines) at  $T_a = 90^\circ\text{C}$  for various preconditioning times:  $t_e = 2^{11}\text{ s}$  ( $\diamond$ );  $2^{13}\text{ s}$  ( $\square$ );  $2^{15}\text{ s}$  ( $\triangle$ );  $2^{17}\text{ s}$  ( $\circ$ );  $2^{19}\text{ s}$  ( $\times$ )

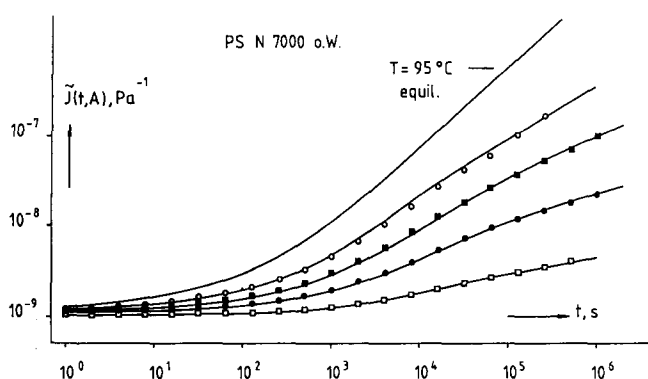


Figure 12 Comparison between experiment (symbols) and theory (drawn lines) after a preconditioning time  $t_e = 2^{13}$  s at various ageing temperatures:  $T_a = 92.5^\circ\text{C}$  ( $\circ$ );  $90^\circ\text{C}$  ( $\blacksquare$ );  $85^\circ\text{C}$  ( $\bullet$ );  $70^\circ\text{C}$  ( $\square$ )

3. calculation of the time-age shift function  $a_s$  according to equation (26) with respect to the prehistory and the ageing conditions desired;
4. application of the shift factors to the equilibrium reference creep curve.

In Figure 11 a comparison is made between experiment (symbols) and theory (solid lines) at the ageing temperature of  $90^\circ\text{C}$ . The experimental values are the same as in Figure 4 as well as the equilibrium creep curve, which was used as reference curve for the calculation of the ageing creep curves. As can be seen, an excellent description of the ageing behaviour is obtained for all preconditioning times. Similarly, good agreement between experiment and theory is seen in Figure 12 for various ageing temperatures. The experimental data are taken from Figure 5 and again the solid lines represent the calculated shape of the ageing creep curves using the equilibrium creep curve at  $95^\circ\text{C}$  as reference curve, as indicated.

The present paper has shown that the free volume seems to be a suitable quantity for describing and predicting volume recovery effects as well as physical

ageing phenomena. It looks promising to follow this approach and to extend the investigations to lower temperatures, other materials<sup>22</sup> and other physical quantities, as shown by Chow<sup>24</sup> for the relationship between the non-equilibrium glassy state and yield stress for amorphous polymers.

Prediction of the mechanical behaviour of polymers is one of the great unsolved problems in the plastics industry and this contribution provides a step in this direction.

## REFERENCES

- 1 Struik, L. C. E. 'Physical Aging in Amorphous Polymers and Other Materials', Elsevier, Amsterdam, 1978
- 2 Schwarzl, F. R., Link, G., Greiner, R. and Zahradnik, F. *Prog. Colloid Polym. Sci.* 1985, **71**, 180
- 3 Kovacs, A. J. *Fortschr. Hochpolym. Forsch.* 1963, **3**, 394
- 4 Greiner, R. and Schwarzl, F. R. *Colloid Polym. Sci.* 1989, **267**, 39
- 5 Turnhout, J. v. 'Thermally Stimulated Discharge of Polymer Electrets', Elsevier, Amsterdam, 1975
- 6 Hopkins, I. L. *J. Polym. Sci.* 1958, **28**, 631
- 7 Haugh, E. F. *J. Appl. Polym. Sci.* 1959, **1**, 144
- 8 Kovacs, A. J., Aklonis, J. J., Hutchinson, J. M. and Ramos, A. R. *J. Polym. Sci., Polym. Phys. Edn* 1979, **17**, 1097
- 9 Greiner, R. PhD Thesis, University of Erlangen, 1987
- 10 Doolittle, A. K. *J. Appl. Phys.* 1951, **22**, 1471
- 11 Hutchinson, J. M. and Kovacs, A. J. in 'The Structure of Non-Crystalline Materials' (Ed. P. H. Gaskell), Taylor and Francis, London, 1977
- 12 Greiner, R. and Schwarzl, F. R. *Rheol. Acta* 1984, **23**, 378
- 13 Link, G. PhD Thesis, University of Erlangen, 1985
- 14 Ferry, J. D. 'Viscoelastic Properties of Polymers', 3rd Edn, Wiley, New York, 1980
- 15 Williams, M. L., Landel, R. F. and Ferry, J. D. *J. Am. Chem. Soc.* 1955, **77**, 4701
- 16 Lang, G. personal communications, Erlangen, 1983
- 17 Feglar, H. personal communications, Erlangen, 1985
- 18 Gabler, H. personal communications, Erlangen, 1986
- 19 Schwarzl, F. R., Greiner, R., Link, G. and Zahradnik, F. in 'Advances in Rheology' (Eds B. Mena, A. Garcia-Rejon and D. Rangel-Nafaile) Univ. Nac. Autonoma de Mexico, Mexico City, 1984, Vol. 1, pp. 211-233
- 20 Kurzendörfer, R. personal communications, Erlangen, 1987
- 21 Grimm, T. personal communications, Erlangen, 1988
- 22 Bilwatsch, D. personal communications, Erlangen, 1986
- 23 Pfandl, W., Link, G. and Schwarzl, F. R. *Rheol. Acta* 1984, **23**, 277
- 24 Chow, T. S. *J. Polym. Sci.* 1987, **25**, 137